

---

**Stanislav SEITL<sup>1</sup>, Viliam VISZLAY<sup>2</sup>, Hector CIFUENTES<sup>3</sup>, Alfonso CANTELI<sup>4</sup>****EFFECTS OF SPECIMEN SIZE AND CRACK DEPTH RATIO ON CALIBRATION CURVES FOR MODIFIED COMPACT TENSION SPECIMENS****Abstract**

The compact tension (CT) test is frequently used to determine fracture properties of metallic materials, such as fracture energy, fracture toughness, crack propagation rate and J-R curves. In the case of cement based composites, a modified compact tension (MCT) specimen can be advantageously used due to the negligible stress concentration arising around the pulling dowel pins during the test. In this work, finite element calculations are used to determine the calibrations curves for the stress intensity factor  $K$ , COD, CMOD and CMOD(4), needed for an accurate determination of the fracture parameters, as a function of the ratio  $a/W$ . Nominal diameters are selected according to the used core bits between 50 mm and 300 mm.

**Keywords**

Modified compact tension test, fracture, concrete, core drill, stress intensity factor, compliance expressions, finite element simulation.

**1 INTRODUCTION**

Many concrete structures are subjected to repeated loadings during their service life, whereby prediction of potential fatigue crack path is crucial for safety evaluation and structural design of relevant components or structures, e.g. bridges, seashore structures, runways, etc. Because of the complex stress distribution on the structure surface, prediction of where surface crack path starts is always a challenge for engineers and research scientists due to their negative effect on durability of concrete when combined with e.g. corrosion of steel bars under chloride penetration and carbonation through these cracks, etc. Furthermore, inspection of crack propagation on surfaces with maximum stress is also significant for predicting the residual fatigue life of concrete structure and for establishing repair schedules of the reinforcement.

For determining the fracture parameters of quasi-brittle materials like concrete, three point bending (3PB), four point bending (4PB) or wedge splitting tests (WST) are used for which the K-calibration and compliance curves are typically determined, see [14],[11].

Among the test configurations mentioned, the 3PB or 4PB specimens are not appropriate for determining the fatigue properties of real constructions, due to the large mass of material required in the specimen preparation, while in the WST test the grips causes troubles under fatigue load, etc.

---

<sup>1</sup> Doc. Ing. Stanislav Seitl, Ph.D., Institute of Physics of Materials, Academy of Sciences of the Czech Republic and Faculty of Civil Engineering, Brno University of Technology, Veveří 331/95, 602 00 Brno, Czech Republic, phone: (+420) 532 290 361, e-mail: seitl@ipm.cz.

<sup>2</sup> Bc. Viliam Vizlay, Faculty of Civil Engineering, Brno University of Technology, Veveří 331/95, 602 00 Brno, Czech Republic, phone: (+420) 532 290 338, e-mail: viliak@centrum.sk.

<sup>3</sup> Associate professor Hector Cifuentes, Ph.D., Escuela Técnica Superior de Ingeniería, Universidad de Sevilla, Camino de los Descubrimiento, s/n, 41092 Sevilla, Spain, phone: (+34) 653 382 232, e-mail: bulte@us.es.

<sup>4</sup> Professor Alfonso F. Canteli, Ph.D., Escuela Politécnica de Ingeniería, Universidad de Oviedo, Campus de Viedques, 33203 Gijón, Spain, phone: (+34) 985 182 054, e-mail: afc@uniovi.es.

As an alternative, the modified compact tension (MCT) test can be recommended for fatigue testing (e.g. to check the residual life) of specimens from concrete constructions due to the round shape of the extracted drilling core samples [11]. Modified compact tension specimens, though with rectangular shape and glued steel plates at the sides, were already used by other authors for studying the influence of the load [15], dynamic fracture of CT specimen [12] or checking the cohesive law [8].

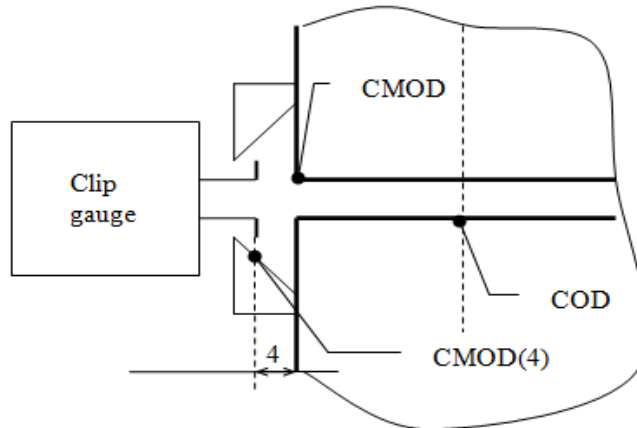


Fig. 1 Detail referred to the measured points of MCT specimen as defined as the COD, CMOD and CMOD(4) positions

Due to the above reported lack in research, a parametrical study of MCT specimens within the framework of linear elastic fracture mechanics (LEFM) is carried out in this work. Note, that though LEFM is not strictly suitable for material like concrete, the fracture toughness and Young's modulus are supposed to be acceptable when taken from the pre-peak branch or during high cycle fatigue loading account given of the small process zone resulting from the stress field at the crack front. The fracture parameters describing the concrete behavior are introduced as stress intensity factor ( $K$ ) and Crack Opening Displacement (COD), Crack Mouth Opening Displacement (CMOD) and Crack Mouth Opening Displacement, the latter at a distance of 4 mm (due to clip gauge) outside the specimen forefront (CMOD(4)), see Fig. 1. The  $K$ -calibration and compliance curves for modified compact tension specimen are prepared for different specimen diameters, which are assumed to correspond with the drilling core [6]. The values of  $K$ -calibration and compliance curves are compared and the values of the coefficients are given in tables.

## 2 THEORETICAL BACKGROUND

The output obtained from the fracture test of concrete is the recorded Load –Displacement diagram, from which the fracture parameters as  $E$ – Young's modulus,  $K_{IC}$ – fracture toughness,  $G_f$ – fracture energy etc. can be determined. On its turn, the fatigue tests provide the COD-N (crack opening displacement versus number of cycles) diagram for constant force, from which the Paris-Erdogan law parameters ( $m$ ,  $C$ ) can be obtained. [3]

The reference dimensions of MCT specimens are  $D$  – diameter,  $W$  – width (according the ASTM  $W=D/1.35$ ),  $a$  – crack length and  $B$  – thickness, all in mm, see in Fig. 2.

The diameter values were selected in order to cover all possible core drilling sizes in the practice, e.g. 50 mm corresponding to 2 inch [2], 100 mm as the standardized Brazilian cylinder size [9],[1], 150 mm as the typical standard specimen size for compressive test [13],[1], and further, 200 mm, 250 mm and 300 mm, see [6].

In the present numerical study,  $\alpha$  (relative crack length) is defined as the ratio of the effective crack length, i.e. the distance between the alignment of the applied force and the crack tip, and the

effective specimen width, i.e. the distance between the alignment of the applied force to the end of the specimen:

$$\alpha = a/W. \quad (1)$$

where:

$a$  – is the crack length [mm] and

$W$  – is the width [mm].

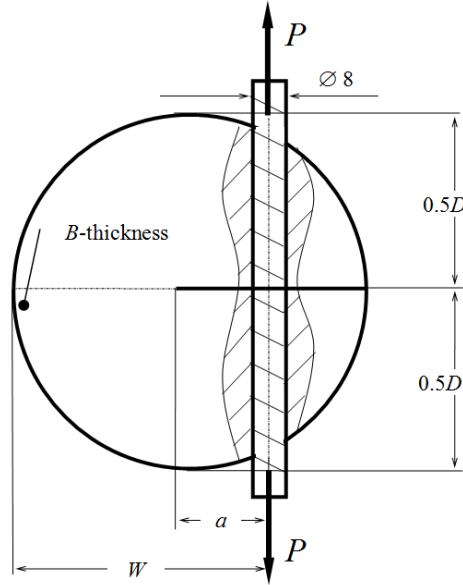


Fig. 2 Sketch of the modified compact tension test (MCT)

According to the fracture mechanics approach [3], the stress field around the crack tip of a two-dimensional crack embedded in an isotropic linear elastic body subjected to normal mode I loading conditions is given by the following expressions [3,16]:

$$\begin{aligned} \sigma_{xx} &= \frac{K_I}{\sqrt{2\pi r}} \cos\left(\frac{\theta}{2}\right) \left[ 1 - \sin\left(\frac{\theta}{2}\right) \sin\left(\frac{3\theta}{2}\right) \right], \\ \sigma_{yy} &= \frac{K_I}{\sqrt{2\pi r}} \left(\frac{\theta}{2}\right) \left[ 1 + \sin\left(\frac{\theta}{2}\right) \sin\left(\frac{3\theta}{2}\right) \right], \\ \tau_{xy} &= \frac{K_I}{\sqrt{2\pi r}} \cos\left(\frac{\theta}{2}\right) \sin\left(\frac{\theta}{2}\right) \cos\left(\frac{3\theta}{2}\right), \end{aligned} \quad (2)$$

where:

$r$  – is the radial coordinate of the polar system in crack tip [mm],

$\theta$  – is the angular coordinate of the polar system in crack tip [rad],

$x, y$  are the coordinate of Cartesian coordinate system in crack tip [mm],

$K_I$  – is the stress intensity factor [MPa m<sup>1/2</sup>],

$\sigma_{xx}, \sigma_{yy}, \tau_{xy}$  – are the stresses for the given axis directions [MPa].

The value of the stress intensity factor for the MCT geometry in linear fracture mechanics is derived from the following formula:

$$K_I = \frac{P}{B\sqrt{W}} B_1(\alpha), \quad (3)$$

where

- $B_1(\alpha)$  – is the dimensionless K – calibration function [-] according to [10],
- $\alpha$  – is the relative crack length [-],
- $B$  – is the thickness of the specimen [mm],
- $W$  – is the width [mm],
- $P$  – is the external load [N].

For the COD values is it so important the knowledge about the thickness of the specimen, in the study cases the calculation was done for plane strain condition, because the used thickness for pilot experiment was 60 mm [7]. The values of COD (crack opening displacement), CMOD (crack mouth opening displacement) and CMOD(4) (crack mouth opening displacement at 4 mm outside the specimen for front) as a function relative crack length  $\alpha$  are introduced in the following:

$$u_y = u_{y0} f(a/W) \quad (4)$$

where

- $f(a/W)$  – is a dimensionless function depending on the measured point as defined, respectively, by COD, CMOD or CMOD(4), and  $u_{y0}$  is given by the expression:

$$u_{y0} = \frac{B_1(\alpha) K_0 (1 + \nu) \sqrt{a}}{2EB\sqrt{2\pi}}, \quad (5)$$

where

- $B_1(\alpha)$  – is the dimensionless geometrical function [-] according to [10],
- $\alpha$  – is the relative crack length [-],
- $B$  – is the thickness of the specimen [mm],
- $W$  – is the width [mm],
- $K_0$  – is the normalized value of stress intensity factor [MPa],
- $E$  – is the Young's modulus [MPa],
- $\nu$  – is the Poisson number [-].

### 3 NUMERICAL SIMULATION

The finite element (FE) software ANSYS [4] is used for numerical calculation of the fracture parameters. Three examples of the specimens handled are shown in Fig. 3, the models of which are arranged from element PLANE82, the smallest one at the crack tip being 0.25 mm. Only one half of the MCT specimen needs to be considered because of the symmetry. At the crack tip, these elements degenerate to triangles with mid-side nodes of element edges pointing to the crack tip and shifted to a one fourth of the position along the element edge in order to introduce the proper  $1/\sqrt{r}$  stress singularity, see command KCALC [4]. The material input data for concrete and steel used in the numerical simulation are the following: Young's modulus  $E_c = 44$  GPa,  $E_s = 210$  GPa and Poisson's ratio  $\nu_c = 0.2$ ,  $\nu_s = 0.3$ , respectively. For the numerical solution, a load  $P = 100$  N is applied. Fig. 4 shows two examples of the MCT finite element models with the corresponding boundary conditions.

The stress intensity factor  $K_I$  values are computed in two different ways, namely, using the stress difference method [18] and the KCALC command [4]. The calculations provided by ANSYS are controlled by means of the results provided by [16][11][14] and [5] (the finite element model was prepared in the CT configuration, the results were checked to obtain less than 1% difference, that the

used model was remodeled to MCT geometry), e.g. with the stress intensity factor for the compact tension specimen calculated as follows:

$$K = \frac{P}{B\sqrt{W}} \frac{(2 + \alpha)}{(1 - \alpha)^{3/2}} (0.886 + 4.64\alpha - 13.32\alpha^2 + 14.72\alpha^3 - 5.6\alpha^4), \quad (6)$$

where

$P$  – is the external load [N],

and  $\alpha$ ,  $B$  and  $W$  have the same meaning as before.

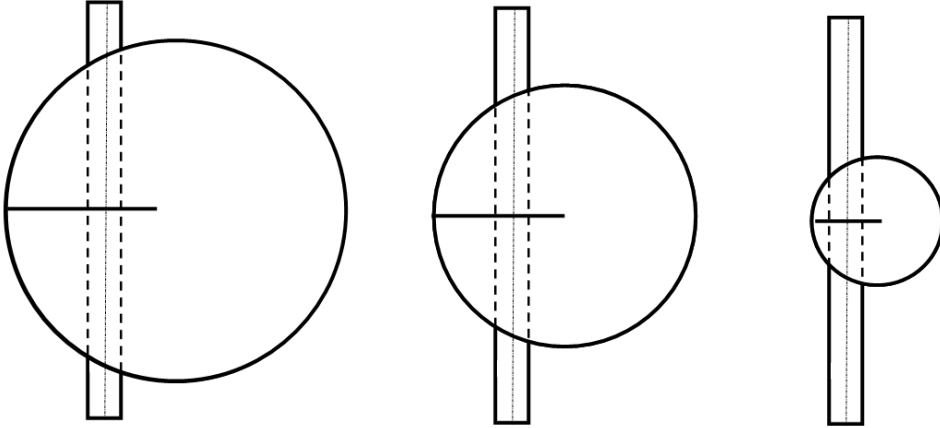


Fig. 3 Sketches of the MCT specimens for the same steel bars and different concrete sample dimension

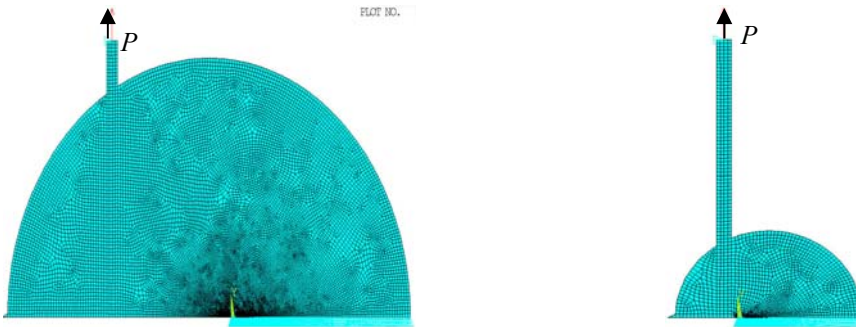


Fig. 4 Examples of the half MCT specimen as finite element model used for determination of the stress intensity factor: a)  $D = 300$ ,  $a/W=0.4$  and b)  $D=100$ ,  $a/W = 0.1$  together with boundary conditions

### 3 RESULTS AND DISCUSSION

Six different MCT specimen configurations are investigated. The numerically calculated values of the normalized stress intensity factor (i.e.  $B_1(\alpha)$ ) for the MCT specimens are summarized in Table 1 and plotted in Fig. 5. The compliance expressions related to the specific measurement location (COD, CMOD and CMOD(4)) for the MCT are presented in Tables 2-4 and shown in Fig. 5.

#### *Stress intensity factor (SIF)*

The SIF is calculated by Eq. (3), where  $B_1(\alpha)$  are the dimensionless K-calibration functions shown in Fig. 5. The symbols are the results obtained from the finite element analysis whereas the full curves are the fitted values. The SOLVER© software routine, available as an additional plug-in

in Microsoft Excel, is utilized to perform the regression analysis of the FEA data. This routine searches the set of values of the fitting factor constants or parameters by minimizing the sum of squares of residuals, i.e., the differences between the actual and the corresponding prediction values. The prediction seems to agree well with the analytical data. The following equation represents the normalized stress-intensity factor  $B_1(a/W)$  for MCT specimen in the range  $0.3 \leq a/W \leq 0.7$  with an accuracy higher than 99.95%.

$$B_1(\alpha) = -68.404 + 804.41\alpha - 3489.7\alpha^2 + 7547.5\alpha^3 - 8034.5\alpha^4 + 3441.5\alpha^5. \quad (7)$$

Table 1 shows the comparison among the dimensionless K-calibration curves  $B_1(a/W)$ , for six different values of the specimen diameter. The results are similar in the interval  $a/W \in (0.3; 0.7)$ , the main difference arising for short cracks in which the boundary effect plays an important role.

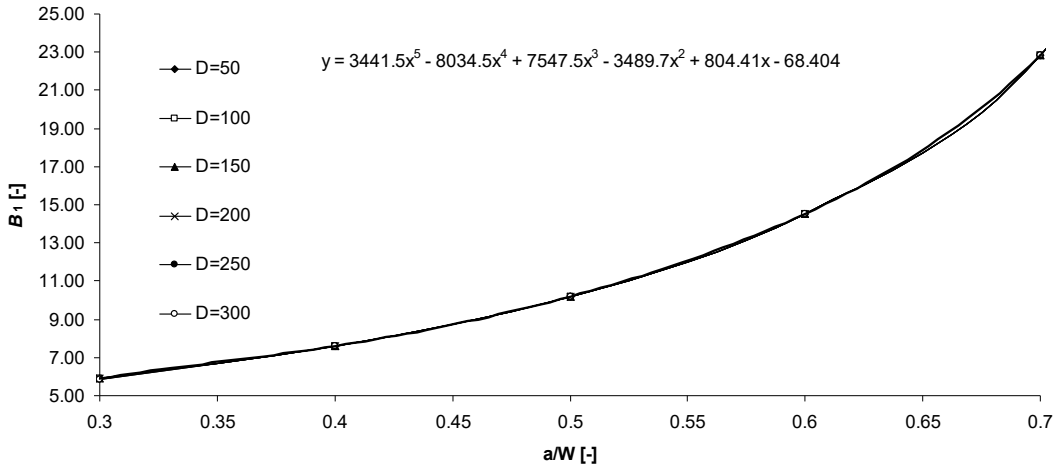


Fig. 5 Dimensional geometry function  $B_1(a/W)$ , for different relative crack lengths for six different  $D = 50, 100, 150, 200, 250, 300$  mm

Table 1: Comparison of dimensionless K-calibration function  $B_1(a/W)$  for selected relative crack lengths for all studied MCT configurations.

$a/W; D$	50	100	150	200	250	300
0.1		4.020	3.885	3.828	3.793	3.766
0.2		4.697	4.675	4.662	4.653	4.645
0.3	5.909	5.885	5.879	5.874	5.872	5.869
0.4	7.600	7.593	7.591	7.589	7.588	7.587
0.5	10.195	10.193	10.192	10.191	10.191	10.191
0.6	14.537	14.536	14.536	14.537	14.536	14.536
0.7	22.834	22.834	22.835	22.835	22.835	22.835
0.8	42.792	42.800	42.800	42.800	42.801	42.801
0.85	66.518	66.553	66.555	66.556	66.557	66.556
0.9	123.298	123.471	123.434	123.481	123.487	123.488

### Compliance function

The displacements at the crack open displacement, crack mouth open displacement and crack mouth open displacement in 4 mm from the relevant location (see Fig. 2) are introduced in this paragraph. Examples of compliance function for COD are shown in Fig. 6. The symbols are the results obtained from finite element analysis and full lines are the fitted values.

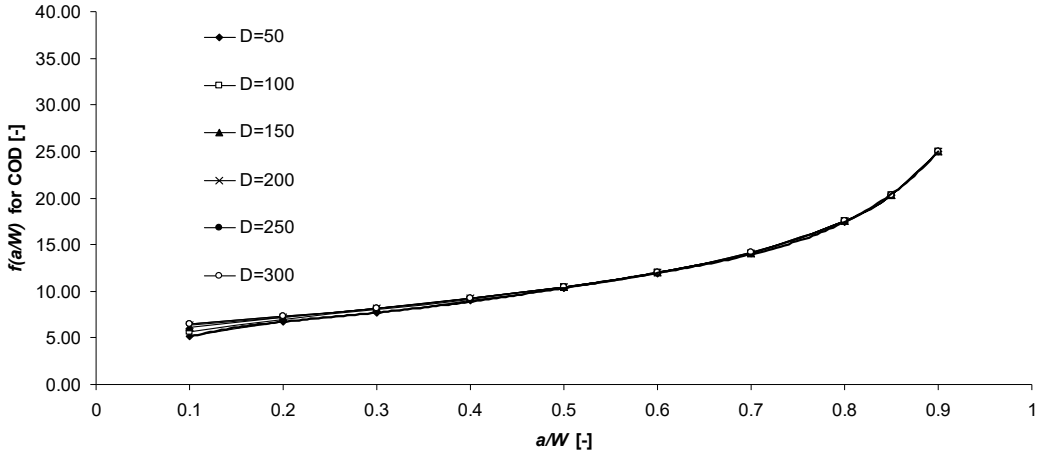


Fig. 6 Comparison among compliance functions ( $COD/2(a/W)$ ) for different relative crack lengths for six different diameters  $D = 50, 100, 150, 200, 250, 300$  mm from finite element data

The displacement is given by eq. (4), whereas  $f(a/W)$  is a polynomial function of  $(C_i)$ , the functional form of which is given by:

$$f(a/W) = C_0 + C_1 \left( \frac{a}{W} \right) + C_2 \left( \frac{a}{W} \right)^2 + C_3 \left( \frac{a}{W} \right)^3 + C_4 \left( \frac{a}{W} \right)^4 + C_5 \left( \frac{a}{W} \right)^5, \quad (7)$$

where

$C_0, C_1, C_2, C_3, C_4, C_5$  are constants obtained through numerical analysis for COD, CMOD, CMOD(4) as reported in Table 2, 3 and 4, respectively.

The equations are valid along the range  $0.2 \leq a/W \leq 0.85$  and have an accuracy higher than 98%.

The obtain curve can be used for experimental campaign for estimation average crack length in each point of load–displacement diagram.

Table 2: Coefficients of dimensionless compliance function from eq. (7) for COD calculation.

$D$ [mm]	$C_0$	$C_1$	$C_2$	$C_3$	$C_4$	$C_5$
50	0.7968	68.639	-326.66	841.37	-1001.5	458.38
100	1.5903	63.639	-303.96	786.85	-941.73	434.4
150	3.0268	50.496	-254.7	696.99	-862.94	407.83
200	3.6088	45.039	-233.6	656.98	-826.25	394.84
250	3.9016	42.334	-223.54	638.76	-810.27	389.41
300	4.0830	40.605	-217.07	627.04	-800.04	385.96

Table 3: Coefficients of dimensionless function from eq. (7) for CMOD calculation

$D$ [mm]	$C_0$	$C_1$	$C_2$	$C_3$	$C_4$	$C_5$
50	-40.1740	519.60	-2025.60	3936.50	-3734.30	1402.30
100	6.4444	75.546	-387.98	1028.90	-1245.40	577.83
150	9.1181	50.708	-294.18	856.84	-1093.80	526.43
200	10.3450	39.331	-250.67	775.29	-1019.90	500.57
250	11.0930	32.593	-225.81	730.36	-980.56	487.25
300	11.6500	27.563	-207.28	696.95	-951.42	477.42

Table 4: Coefficients of dimensionless function from eq. (7) for CMOD(4) calculation.

$D$ [mm]	$C_0$	$C_1$	$C_2$	$C_3$	$C_4$	$C_5$
50	-42.538	559.490	-2183.90	4244.9	-4027.3	1512.40
100	7.1252	77.966	-403.03	1069.9	-1295.4	601.02
150	9.6851	51.248	-300.11	876.63	-1120.4	539.60
200	10.811	39.358	-253.68	787.46	-1037.5	509.61
250	11.488	32.420	-227.51	738.8	-993.49	494.10
300	11.994	27.289	-208.22	703.13	-961.45	482.88

## 6 CONCLUSIONS

This study is prepared to support the experimental campaign that was done on concrete specimens with steel bars for load application. The CT compliance function could not be used due to material interface (steel – concrete) and due to different distance of load application.

The influence of specimen size and crack depth ratio on the calibration curves for modified compact tension specimen is analyzed using linear elastic fracture analysis. The specimen geometry allows the user to obtain efficiently crack growth data under a displacement controlled test. Finite element analysis is used to obtain the stress-intensity factors and displacements over a wide range of crack/length to width ratios ( $a/W$ ).

Expressions for estimating values of the stress intensity factor, and crack length from measurement of crack opening displacement, crack mouth opening displacement and crack mouth opening displacement in 4 mm (compliance) are provided for the MCT specimen geometry.

## ACKNOWLEDGMENT

This paper has been worked out under the “National Sustainability Programme I” project “AdMaS UP – Advanced Materials, Structures and Technologies” (No. LO1408) supported by the Ministry of Education, Youth and Sports of the Czech Republic. The authors acknowledge financial support of the project No. FAST-S-15-2774 (BUT), project No. 15-07210S (Czech Science Foundation), BIA2013-48352-P (Ministry of Economy and Competitiveness of Spain) and SV-PA-11-012 (Asturian Regional Government).

## REFERENCES

- [1] AHMED, M.U., RAHMAN, A., ISLAM, M.R., TAREFDER, R.A. Combined effect of asphalt concrete cross-anisotropy and temperature variation on pavement stress-strain under dynamic loading, *Construction and Building Materials*. 2015, Volume 93, pp. 685–694.
- [2] ALDAZABAL, J., MARTÍN-MEIZOSO, A., MARTÍNEZ-ESNAOLA, J.M., Experimental measurement of Mode I & II critical stress intensity factor of stones. *Anales de mecanica de la fractura* 2015, Volume 32, pp. 154–159, ISSN: 0213-3725.
- [3] ANDERSON, T.L. *Fracture mechanics fundamentals and applications* 1991, CRC Press ISBN: 978-0849316562.
- [4] ANSYS: Příručka ANSYS Workbench 2012, Česká technika – nakladatelství ČVUT, ISBN: 978-80-01-05175-7.
- [5] ASTM, E647-13a, Standard Test Method for Measurement of Fatigue Crack Growth Rates, ASTM International, West Conshohocken, PA, 2013, [www.astm.org](http://www.astm.org).
- [6] CIFUENTES, H., LOZANO, M., HOLUŠOVÁ, T., MEDINA, F., SEITL, S., CANTELI, F., Applicability of a modified compact tension specimen for measuring the fracture energy of concrete, *Anales de Mecánica de la Fractura*, Vol. 32 (2015) pp. 208–213.
- [7] European Standard EN 12390-1:2012 – Testing hardened concrete – Part 1: Shape, dimensions and other requirements for specimens and moulds 2012.
- [8] FERNANDEZ-CANTELI, A., CASTAÑÓN, L., GARCIA-NIETO, B., HOLUSOVA, T., SEITL, S. Determining fracture energy parameters of concrete from the modified compact tension test, *Frattura ed Integrità Strutturale*, (2014), Volume 30, pp. 383–393; DOI: 10.3221/IGF-ESIS.30.46.
- [9] KOURKOULIS, S.K., MARKIDES, CH. F., CHATZISTERGOS, P.E., The standardized Brazilian disc test as a contact problem, *International Journal of Rock Mechanics & Mining Science*. 2013, Volume 57, pp. 132–141, DOI: <http://dx.doi.org/10.1016/j.ijrmms.2012.07.016>
- [10] LEEVERS, P. S., RADON, J. C. *Inherent stress biaxiality in various fracture specimen geometries*. *International Journal of Fracture*, 1982, pp. 311–325.
- [11] MURAKAMI, Y. *Stress intensity factors hand book*. Pergamon Press, 1987.
- [12] OŽBOLT, J., BOŠNJAK, J., SOLA, E., Dynamic fracture of concrete compact tension specimen: Experimental and numerical study, *International Journal of Solids and Structures*, 2013, Volume 50, pp. 4270–4278
- [13] RILEM Recommendations for the Testing and Use of Constructions Materials, CPC 4 Compression test on concrete, 1975.
- [14] TADA, H., PARIS, P.C. and IRWIN, G.R. *The stress analysis of crack handbook*, The American Society of Mechanical Engineers Three Park Avenue, New York, NY 10016, ISBN: 1-86058-304-0.
- [15] VESELÝ, V., SOBEK, J. Numerical study of failure of cementitious composite specimen in modified compact tension fracture test, *Sborník vědeckých prací Vysoké školy báňské-Technické univerzity Ostrava*, 2013, Volume 13(2), pp. 209–2016.
- [16] VISZLAY, V. Numerical support for analysis of the fatigue behavior of cement based composites, Bachelor thesis BUT Brno 2015, p. 28-33 (in Slovak).
- [17] WILLIAMS, M.L. On the stress distribution at the base of stationary crack, *ASME Journal of Applied Mechanics* 1957, 24, 109–114. ISSN: 0021-8936.
- [18] YANG B., RAVI-CHANDAR K. Evaluation of elastic T-stress by the stress difference method. *Engineering Fracture Mechanics*, 1999, Volume 64, pp. 589–605.

**Reviewers:**

MSc. Pablo López Crespo, Ph.D., Department of Civil and Materials Engineering, University de Malaga, Spain.

Ing. Aleš Materna, Ph.D., Department of Materials, Faculty of Nuclear Sciences and Physical Engineering, Czech Technical University in Prague, Czech Republic.